Biochimica et Biophysica Acta, 1143 (1993) 215–222

BBABIO 43844

Kinetic characterization of the ATP-dependent proton pump in bacterial photosynthetic membranes: a study with the fluorescent probe 9-amino-6-chloro-2-methoxyacridine

Valeria Fregni and Rita Casadio

Laboratory of Biochemistry and Biophysics, Department of Biology, University of Bologna, Bologna (Italy)

(Received 30 November 1992)

Key words: ATP synthase; Enzyme kinetics; Proton translocation; pH difference determination; Fluorescent probe; Energy coupling

In bacterial photosynthetic membranes the generation of a transmembrane ΔpH coupled to ATP hydrolysis is detected by monitoring the quenching of fluorescence of the monoamine 9-amino-6-chloro-2-methoxyacridine (ACMA), induced in the dark upon addition of the substrates of the ATPase reaction. When Mg-ATP is the reaction complex, kinetic analysis of the hydrolytic and proton pumping activities indicates a similar affinity for the substrate ($K_m = 0.20 \pm 0.05$ mM) and maximal rates of ΔpH generation and ATP hydrolysis of 0.37 ± 0.05 ΔpH units s^{-1} and 10 ± 2 nmol ATP hydrolyzed s^{-1}. (μmol BChl)$^{-1}$, respectively. A comprehensive investigation of the effects of previously known modulators and/or effectors of the ATPase activity on the proton pump shows that in bacterial photosynthetic membranes, ΔpH generation is strictly regulated in parallel with ATP hydrolysis. These results validate the use of ACMA fluorescence to monitor transmembrane ΔpH of 0.1–1.5 units and to detect F_1–F_0 functional interactions.

Introduction

Bacterial photosynthetic membranes (chromatophores) are endowed in the dark with a manifest ATPase activity which is coupled to the generation of a transmembrane electrochemical potential difference for protons ($\Delta\tilde{\mu}_{H^+}$) [1]. These inside-out membrane systems are suited to characterize mechanisms of energy coupling between the hydrolytic and the proton pumping activities of the membrane-bound ATPase complex [2] and to test models of energy transduction [3–5]. The H^+-ATPase is of the F_1–F_0 type and in this respect is similar to its counterpart in energy-conserving membranes from other sources. The F_1 sector contains five different subunits, named α, β, γ, ϵ and δ, with a likely stoichiometry of 3:3:1:1:1, and the nucleotide binding sites [6–8]. The membrane-embedded F_0 part comprises four polypeptides (with an unknown stoichiometry) [9], similar to what is found in the transmembrane complex of the ATPase of chloroplasts from higher plants [10], and acts as a transmembrane proton pump [11].

Several studies from our and other laboratories have extensively characterized regulatory phenomena of the membrane-bound H^+-ATPase in chromatophores and other photosynthetic systems (for reviews, see Refs. 12–14). In chromatophores, these include activation of the ATPase activity by light [15] or artificially induced transmembrane $\Delta\tilde{\mu}_{H^+}$ [16], modulation by anions and divalent cations [17], and capability of hydrolyzing different triphosphate nucleotides (for a review, see Ref. 12). The divalent cation–triphosphate nucleotide complex is the substrate for the ATPase reaction [12], while only MgATP hydrolysis is coupled to proton translocation across the membrane sector [18,19]. The β subunit seems to play a major role in the catalytic cycle, most likely containing both catalytic and regulatory site(s)

Correspondence to: R. Casadio, Department of Biology, V. Irnerio 42, 40126-Bologna, Italy.

Abbreviations: ACMA, 9-amino-6-chloro-2-methoxyacridine; F_0 and F_1, proton translocating and catalytic moieties of the bacterial photosynthetic ATPase; $\Delta\tilde{\mu}_{H^+}$, transmembrane electrochemical potential difference for protons; ΔpH, transmembrane proton concentration difference; $\Delta\psi$, transmembrane potential difference; Tricine, *N*-[2-hydroxy-1,1-bis(hydroxymethyl)methylglycine; ATP, adenosine 5′-triphosphate; ADP, adenosine 5′-diphosphate; ITP, inosine 5′-triphosphate; IDP, inosine 5′-diphosphate; P_i, inorganic phosphate; BChl, bacteriochlorophyll; NAD and NADH, oxidized and reduced β-nicotinamide adenine dinucleotide; EDTA, [ethylenedinitro]tetraacetic acid; EGTA, [ethylene-bis(oxyethylenenitrilo)]tetraacetic acid; DCCD, *N*,*N*′-dicyclohexylcarbodiimide; CCCP, carbonyl cyanide-*m*-chlorophenylhydrazone.

[19]. In chloroplasts, it is also suggested that the δ subunit, located at the interface between F_1 and F_0, plays a key role in the coupling mechanism between the reaction cycle and the transmembrane proton flow [20].

Although these observations indicate a close relationship between the catalytic and transmembrane sectors of the ATPase complex, a quantitative analysis of the functional interactions of the F_1 and F_0 parts is lacking both in chromatophores and in other types of energy-conserving membranes.

Recently, we proposed the use of the quenching of ACMA fluorescence to detect transmembrane ΔpHs of low extents (in the range of 0.1–1.5 ΔpH units) by developing a model, which after correcting for membrane–probe interactions, accounts for the relationship between artificially induced transmembrane ΔpHs and the quenching of fluorescence [21]. In this paper, we validate the use of this method to monitor transmembrane pH differences coupled to ATP hydrolysis and characterize the kinetic parameters of the proton pumping activity in relation with those of the hydrolytic reaction, under different experimental conditions. The results demonstrate that the proton pumping activity is modulated simultaneously with modulation of the ATPase reaction at the catalytic and/or regulatory sites.

Materials and Methods

Materials

Chromatophores were obtained by mechanical rupture of a green strain of the photosynthetic bacterium *Rhodobacter capsulatus*, harvested at the late logarithmic phase of growth, as previously described and kept at −14°C in a glycerol-containing buffer at pH 7.5 (60 : 40 (v/v), 50 mM sodium glycylglycine) [22]. Adenosine 5′-triphosphate, Tricine, oligomycin, venturicidin, nigericin and valinomycin were purchased from Sigma (St. Louis, MO, USA). ACMA was purchased from Molecular Probes (Eugene, OR, USA). All other chemicals, including $MgCl_2$ and Na_2SO_3 were reagent grade.

Spectroscopic determinations

The concentration of bacteriochlorophyll (BChl) in the chromatophore populations was determined, following extraction in polar solvents (acetone/methanol, 7:2 v/v), and using an extinction coefficient of 75 cm^{-1} mM^{-1} at 775 nm, as already described [23].

ATP was dissolved in 20 mM sodium-Tricine buffer and the pH was adjusted to 6.8 with NaOH. Its concentration was enzymatically determined following NADP reduction at 340 nm, and was usually found to be 5–10% less than that gravimetrically measured. The ADP contamination of the ATP solutions was enzymatically measured as well, following NADH oxidation at 340 nm, and found to range from 1 to 5% of the ATP concentration [24]. The contamination of inorganic phosphate, as detected after complexation with molybdate reagent [25], was also 1–5% of the ATP amount.

The concentrations of endogenous Ca and Mg ions in chromatophores were spectroscopically detected after complexation of Mg^{2+} with Titan yellow and Ca^{2+} with cresolphthalein complexone [26,27]. In different chromatophore populations, the divalent ion to BChl molar ratios were about 6 and 1 for Mg^{2+} and Ca^{2+}, respectively.

Measurement of the ATPase activity

The rate of ATP hydrolysis was measured by detecting the inorganic phosphate released in the supernatant during the ATPase catalytic cycle, as previously described [22]. The assay routinely contained in 1 ml final volume: 50 mM Na-Tricine (pH 8.5), 50 mM KCl, 0.2 mM sodium succinate, 5 μM ACMA, 2 μM valinomycin, and chromatophores corresponding to a BChl concentration of 20 μM. Sodium succinate was added to buffer the ambient redox potential. Ca^{2+} ions, present in the chromatophore suspension, were chelated with EGTA and added at a one-to-one molar ratio with the divalent cation concentration (routinely in the range of 20–50 μM, depending on the chromatophore preparation). The reaction was performed in the dark and started by addition of ATP at a fixed concentration. Mg^{2+} ions were added, when necessary, to the assay medium as $MgCl_2$ and the total Mg^{2+} concentration (evaluated by considering also the endogenous Mg^{2+} content) was equimolar to that of ATP or higher, depending on the experimental conditions. When at low substrate concentrations, the endogenous Mg^{2+} content in chromatophores was higher than that of the MgATP complex (see above), excess Mg^{2+} ions were removed by chelating with equimolar amounts of EDTA.

For each concentration of the substrate, the amount of phosphate released was a linear function of the reaction time for at least 2 min, so that the initial rate of ATP hydrolysis was evaluated by extrapolating at $t = 0$ the slope of the straight line relating P_i concentration and time. This was also detected by measuring the ATP hydrolase activity coupled to the reaction of the pyruvate kinase and lactate dehydrogenase, and by spectroscopically following the oxidation of NADH at 340 nm as described previously [28]. No difference was observed between the two methods.

Similar experiments were also done by adding the substrate in the presence of oligomycin, or venturicidin, known inhibitors of the ATPase in these membranes, so that the oligomycin- or venturicidin-insensitive reaction rate was also detected and subtracted from the previous ones. This activity ranged from 20 to 30% of the total one. Final concentrations of oligomycin

and venturicidin were 10 and 2 μM, respectively. All the data shown in this work refer to the oligomycin-sensitive ATPase activity. No difference was noted when venturicidin was used as inhibitor of the ATPase. Temperature was kept at 27 ± 1°C. Each experiment was performed in triplicate and the average value and mean error calculated therefrom.

Measurement of the proton pumping activity

The fluorescence of ACMA was measured using a Jasco P450 fluorimeter, with excitation and emission at 390 and 510 nm, respectively [21]. The apparatus is described elsewhere [29]. The assay medium was the same as that used for the ATPase reaction, except that the final volume was 2 ml. ACMA was added at a final concentration of 5 μM as ethanolic solution. The ethanol content in the assay medium was 0.1%. The concentration of the probe did not affect the rate of ATP hydrolysis in the range of 0.1–10 μM. The quenching of fluorescence was induced upon ATP addition to the assay medium under continuous mixing, in a thermostated cuvette. Measurements of the quenching of ACMA fluorescence were performed at 27 ± 1°C. Calibration of the quenching of ACMA fluorescence in terms of ΔpH units was performed by imposing artificially induced ΔpH levels of known extents to the chromatophore membranes, as previously described [21].

Evaluation of the substrate concentration

The concentration of the substrates used for measuring the rate of ATP hydrolysis and ΔpH generation were calculated by considering all the multiple equilibria which exist in solutions at a given pH and ionic strength. With the root-finding routine of Newton-Raphson [30], numerical solutions to the following equation were computed:

$$Mg_T = X[1 + ATP_T/(A + X) + ADP_T/(B + X) + AMP_T/(C + X)] \quad (1)$$

where:

$Mg_T = [Mg_T]$ present in the assay

$X = [Mg^{2+}]$ free in solution.

$A = e/(a + b)$

$e = [1 + 10^{(pH - pK_{ATP^{4-}})} \times (1 + [K^+]K_{ATPK} + [Na^+]K_{ATPNa})]$

$a = K_{ATPHMg}$

$b = K_{ATPMg} \cdot 10^{(pH - pK_{ATP^{4-}})}$

$B = f/(c + d)$

$f = [1 + 10^{(pH - pK_{ADP^{3-}})}(1 + [K^+]K_{ADPK} + [Na^+]K_{ADPNa})]$

$c = K_{ADPHMg}$

$d = K_{ADPMg}10^{(pH - pK_{ADP^{3-}})}$

$C = g/i$

$g = [1 + 10^{(pH - pK_{AMP^{2-}})}(1 + [K^+]K_{AMPK} + [Na^+]K_{AMPNa})]$

$i = K_{AMPMg}10^{(pH - pK_{AMP^{2-}})}$

$[Na^+]$, $[K^+]$ are the Na^+ and K^+ ion concentrations present in the assay.

Eqn. 1 can be deduced by considering all the multiple equilibria of the ion–adenine nucleotide complexes which exist in solution at a given pH, ionic strength and temperature [31,32], and the mass balance to the total Mg^{2+} concentration.

The stability constants used, as reported in the literature [33–37], are listed in Table I.

With Eqn. 1, the effective concentration of $MgATP^{2-}$ can be calculated also when the initial ADP and/or AMP concentrations are negligible, as in the experiments described in the following.

Curve fitting and kinetic analysis

Curve fitting was performed using a non-linear least square minimization routine based on a gradient-expansion algorithm, as described by Bevington [38]. Kinetic parameters were calculated therefrom, and their standard deviations were obtained as the square root of the diagonal elements of the error matrix [38].

Results

Measurements of ATP-induced ΔpH

In the dark and in the presence of K^+-valinomycin (to equilibrate K^+ concentration through the membrane phase), addition of MgATP to chromatophore suspensions previously equilibrated with ACMA, promotes a transient quenching of the probe fluorescence, until a steady-state value is attained, as shown in Fig. 1. The initial level of fluorescence is then restored by adding to the membrane suspension inhibitors of the ATPase complex, such as oligomycin, venturicidin and DCCD. Alternatively, the fluorescence can be restored by adding nigericin or CCCP, or, as previously shown, by chelating Mg ions with equimolar amounts of EDTA

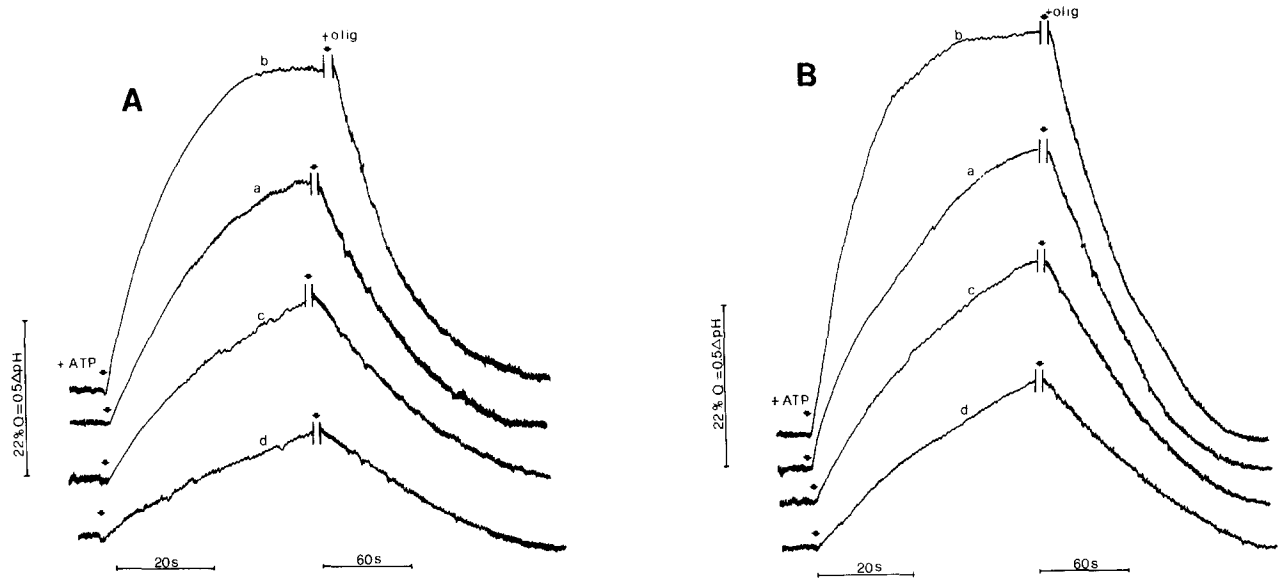

Fig. 1. Quenching of ACMA fluorescence induced in the presence of dark adapted photosynthetic chromatophores upon addition of the substrate for the membrane-bound ATPase complex under different experimental conditions. (A) $[MgATP^{2-}] = 0.101$ mM. Curve a: control experiment; curve b: in the presence of 0.45 mM Na_2SO_3; curve c and curve d: in the presence of 0.65 and 2.5 mM free Mg^{2+}, respectively. Both the substrate and the free Mg^{2+} concentrations are evaluated with Eqn. 1. The final concentration of oligomycin (+olig) was 10 μM. (B) $[MgATP^{2-}] = 0.386$ mM. Legends for curves are as in Fig. 1A.

[18]. Both the initial rate and the extent of the quenching of ACMA fluorescence can be affected by modulating the substrate concentration in the absence or in the presence of known effectors of the hydrolytic activity (Fig. 1A, B), such as free Mg ions and Na_2SO_3. These results clearly indicate that the observed quenching of ACMA fluorescence is related to the ATP-induced proton pumping activity of the membrane-bound ATPase complex.

The quenching of ACMA fluorescence can be used to evaluate the time course of ΔpH formation provided that proper calibration curves are used (Fig. 2). In these experiments, ΔpHs of known extents are artificially induced in chromatophore membranes under the same experimental conditions used above. The dependence of ΔpH on the correspondent quenching (Q) of fluorescence is fitted with the following equation:

$$\Delta pH = A[Q/(B-Q)] \exp[Q/(B-Q)+C] \quad (2)$$

where A, B and C are three empirical fitting parameters. It was previously shown that this dependence is also obtained when the interaction of the probe with the chromatophore membranes is evaluated and included in a model in which the transmembrane ΔpH is determined from the distribution ratio of the inner to the outer concentrations of free neutral monoamine [21]. The A, B and C values obtained by fitting the data presented in Fig. 2 were 4.6, 165 and $-2.3 \cdot 10^{-2}$, respectively, and were not affected when the calibration curve was performed in the presence of ATP, Mg^{2+} and sulphite ions in the range of concentrations used in this work.

TABLE I

Stability constants used for the evaluation of the substrate concentrations

Stability constants of the different ion–adenine nucleotide complexes are evaluated at pH 8.5, 0.1 M ionic strength, and 25°C [30–33].

$K_{ATPMg^{2-}} = 42658$	$K_{ADPMg^{1-}} = 2754$	$K_{AMPMg} = 89$
$K_{ATPHMg^{1-}} = 724$	$K_{ADPHMg} = 100$	
$K_{ATPK^{3-}} = 14$	$K_{ADPK^{2-}} = 5.9$	$K_{AMPK^{1-}} = 4.3$
$K_{ATPNa^{3-}} = 15$	$K_{ADPNa^{2-}} = 4.5$	$K_{AMPNa^{1-}} = 3.2$
$pK_{ATP} = 7.05$	$pK_{ADP} = 6.78$	$pK_{AMP} = 6.47$

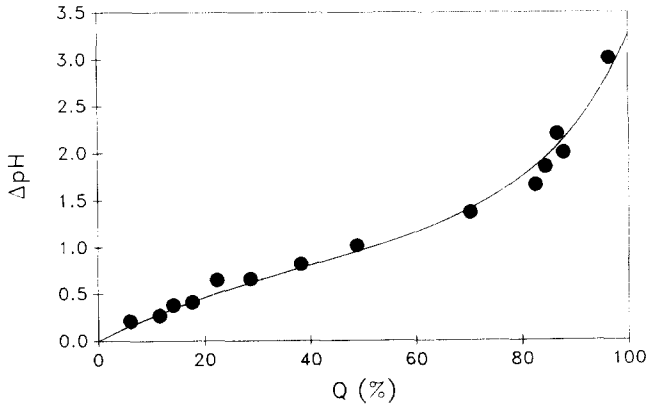

Fig. 2. Calibration of the quenching of ACMA fluorescence in terms of ΔpH. Experimental conditions are described in Materials and Methods. BChl and ACMA concentrations are 20 and 5 μM, respectively. Curve fitting of the experimental data points is performed according to Eqn. 2.

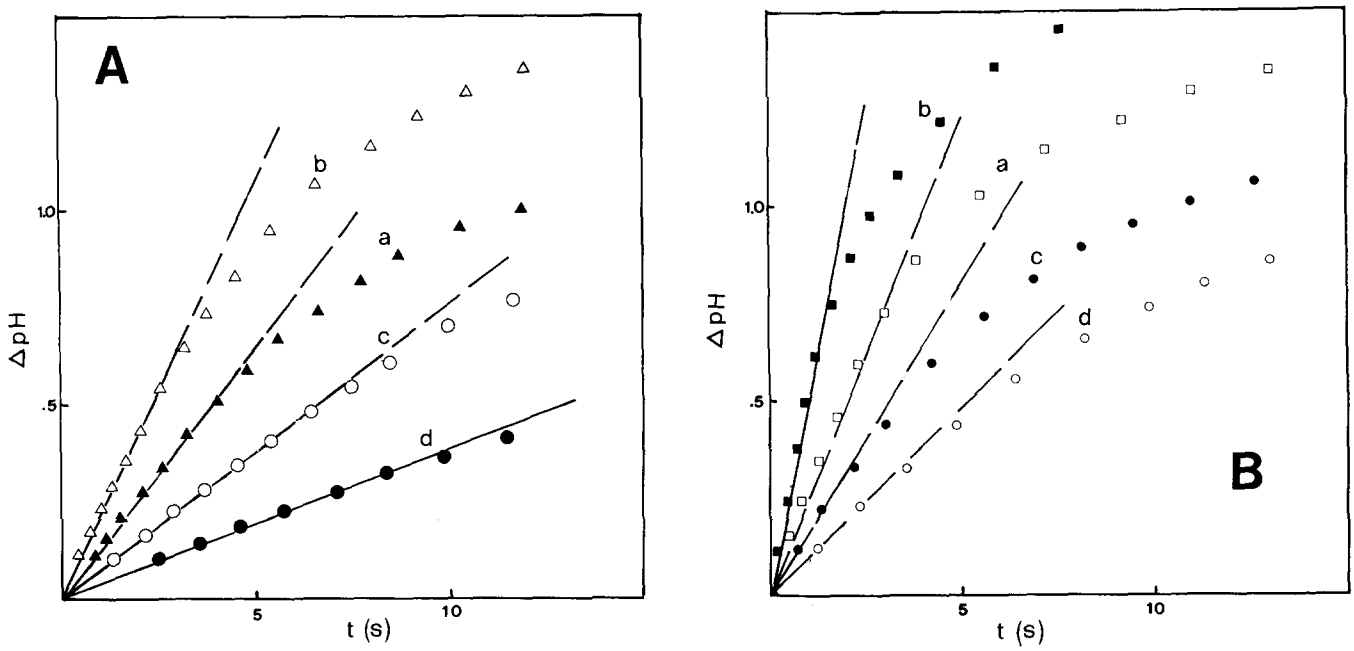

Fig. 3. Time-course of ΔpH formation coupled to ATP hydrolysis in dark-adapted photosynthetic chromatophores. ΔpH is evaluated as a function of time according to Eqn. 2 in A and B from the experiments shown in Fig. 1A and B, respectively. Legends for curves are as in Fig. 1A and B.

By means of Eqn. 2 it was possible to evaluate ΔpH at different times from the traces shown in Fig. 1. The results are shown in Fig. 3A and B. It appears that ΔpH is a linear function of time in the range from about 1 to 10 s, depending on the substrate concentration and experimental conditions. This observation allows to interpolate the results with a straight line and to extrapolate this dependence at $t = 0$. The slope of this linear function is a measure of the initial rate of ΔpH formation (Δṗ H) and is used for kinetic analysis. It must also be noted that during the early enzyme turnovers the total buffering power of the different samples is constant, and the Δṗ H values thus obtained can be used to evaluate the kinetic parameters of the proton pump.

Kinetic analysis of the hydrolytic and proton pumping activities

In Fig. 4A and B, the hydrolytic and proton pumping activities are compared at the different concentrations of the substrates of the ATPase reaction. In the presence of K^+-valinomycin, the thermodynamic back pressure of the electrical transmembrane potential difference on the hydrolytic activity is prevented. Under

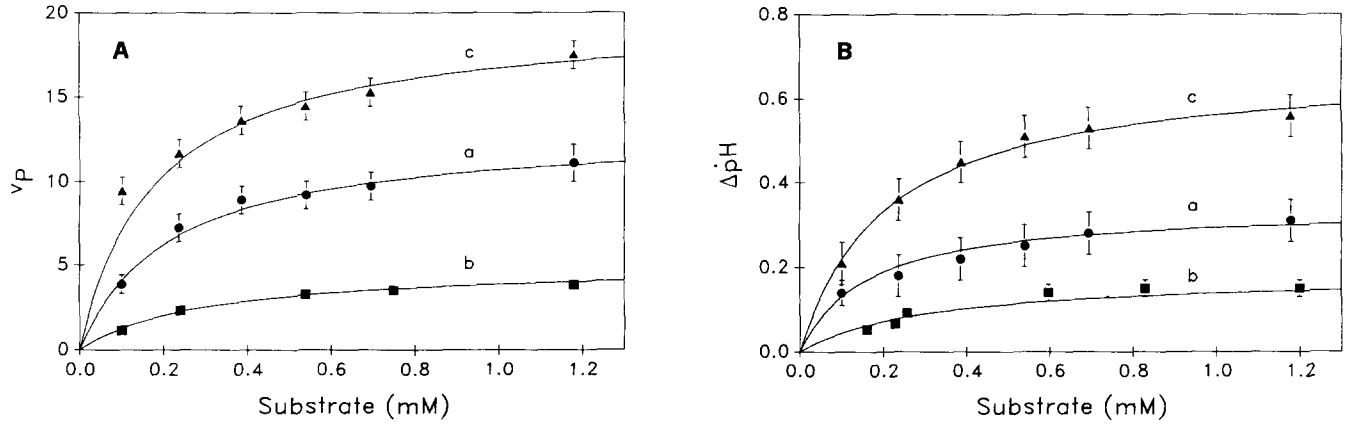

Fig. 4. Kinetic analysis of the ATPase and proton pumping activities in dark-adapted photosynthetic chromatophores under different experimental conditions. In both A and B, curve a: control experiment; curve b: MgITP is used as a substrate for the ATPase reaction; curve c: in the presence of 0.45 mM Na_2SO_3. Substrate concentrations are evaluated according to Eqn. 1. The stability constants for MgITP and MgIDP are the same as those shown in Table I for MgATP and MgADP [37]. The rate of the oligomycin-sensitive ATP hydrolysis (v_p) is measured as nanomol ATP hydrolyzed s^{-1} (μmol BChl)$^{-1}$. Δṗ H, the rate of ΔpH formation, is measured as ΔpH s^{-1}.

TABLE II

Kinetic parameters of the ATPase and proton pumping activities catalyzed by the F_1F_0 enzyme complex in membranes from photosynthetic bacteria

Conditions	v_p		$\Delta\dot{p}H$	
	V_{max} [a]	K_m (mM)	V_{max} (ΔpH s^{-1})	K_m (mM)
MgATP	13 ±1	0.22±0.06	0.34±0.06	0.16±0.09
+[$MgCl_2$] 0.63 mM	13 ±2	0.46±0.04	0.3 ±0.1	0.5 ±0.3
+[$MgCl_2$] 1.25 mM	13 ±1	0.74±0.06	0.3 ±0.1	0.7 ±0.3
+[$MgCl_2$] 2.50 mM	13 ±3	1.2 ±0.5	0.3 ±0.1	1.2 ±0.5
+[$MgCl_2$] 5.00 mM	15 ±9	2.0 ±0.3	0.3 ±0.1	2.0 ±0.9
+[Na_2SO_3] 0.45 mM	20 ±1	0.18±0.04	0.68±0.07	0.21±0.07
MgITP	5.0±0.6	0.29±0.07	0.18±0.02	0.3 ±0.1

[a] (nmol ATP hydrolyzed s^{-1} (μmol BChl)$^{-1}$)

these conditions, the affinity of the hydrolytic activity for the substrate is not affected, while the maximal velocity is increased about 30% as compared to control experiments (data not shown). It is evident that, under these conditions, both activities are kinetically related to the substrate concentrations by the Michaelis-Menten hyperbolic function (less χ square) and show a similar affinity.

This is also observed when MgITP is used as a substrate of the hydrolytic activity. The effect on the kinetics of hydrolysis is a slight increase of the K_m and a decrease of V_{max}. Notably, a similar effect is also observed on the activity of the proton pump (curve b in Fig. 4A and B; see also Table II).

The effects of anions on the hydrolytic activity of the ATPase of chromatophores was tested before [17]. The most effective activator is sulphite, even when used at rather low concentrations (0.45 mM), as in our experiments. In the presence of sulphite, the dependence of the rate of ATP hydrolysis on the concentration of the substrate is still fitted to a hyperbolic function, as shown in Fig 4A. The K_m is similar to that determined in the absence of the anion, while V_{max} increases up to 2-fold the value measured in control experiments (Table II). A parallel activation is also noted in the proton pumping activity (Fig. 4B).

Mg ions, in excess with respect to MgATP, competitively inhibit the hydrolytic activity [12]. This is confirmed also in our experiments when the effect of Mg ions on both activities is measured. The data are shown in Fig. 5A and B. By curve fitting to a Dixon plot (v_p^{-1} vs. concentration of free inhibitor), a K_i of (0.5 ± 0.1) mM is evaluated for both activities (data not shown).

A summary of the kinetic constants of the ATPase and proton pumping activities is shown in Table II.

Discussion

A method is presented here to characterize proton pumping activity coupled to ATP hydrolysis in photosynthetic bacterial membranes. The method is, however, of general use and can be applied to detect ΔpH generation in energy-conserving natural and co-reconstituted membranes, provided that the polarity for proton flux is similar to that of bacterial chromatophores, namely inside-out with respect to the whole cell.

ACMA has been extensively used as a qualitative indicator of transmembrane proton flux in biomem-

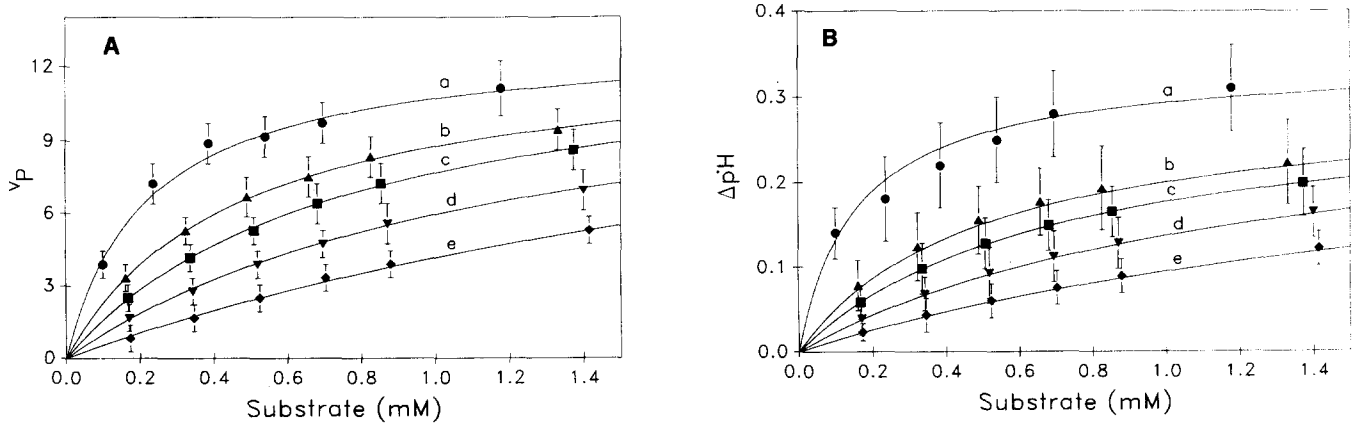

Fig. 5. Kinetic analysis of the ATPase and proton pumping activities in dark-adapted photosynthetic chromatophores as a function of the increasing concentrations of free Mg^{2+}. In both A and B curve a: control experiment; curve b–e: in the presence of 0.63, 1.25, 2.5 and 5 mM free Mg^{2+}, respectively. Concentrations are evaluated according to Eqn. 1.

branes relevant in bioenergetics [39]. We have recently characterized the properties of this dye and its interaction with the membrane phase [21]. Under the experimental conditions used in this paper, it was measured that about 75% of the total amount of ACMA added to the chromatophore suspension binds to the dark adapted membranes, also when the extent of ΔpH, if present, is ≤ 0.1, as due to the Donnan potential in the dark at 0.1 M ionic strength [40].

As previously discussed [21], a model based on the equilibrium distribution of the amine between two bulk phases at different pH levels [41] can predict the S-shaped dependence of ΔpH vs. quenching of fluorescence reported in Fig. 2, provided that binding is included by determining the adsorption isotherm of the probe on the membrane [21]. According to this model, it can be calculated that when the quenching ranges from 1 to 95% of the initial level of fluorescence, the amount of free ACMA in solution (outer and inner volumes) decreases from 25 to 1% of the total amount, the remainder being adsorbed on the total adsorbing surface of the membrane. Concomitantly, the amount of ACMA free in the inner osmotic space changes from $9 \cdot 10^{-4}$ to 10^{-1}% of the total amount of probe added to the assay medium. The main feature of this model is that the probe remains strongly adsorbed on the membrane interfaces even in the presence of ΔpHs as high as 2–3 units, as are those artificially induced by means of acid to basic pH transitions. Any binding promoted by ΔpH formation is negligible in terms of mass displacement from the outer to the inner side of the membrane. Under these conditions, the contribution to the total fluorescence from the molecules free in the inner aqueous volume can be neglected and the quenching observed would be due to partitioning of the probe in the membrane phase, characterized by a low dielectric constant [21].

Based on these considerations, the use of the calibration curve shown in Fig. 2 accounts for membrane–probe interactions. A major advantage in using ACMA as compared to other ΔpH responding probes is the sensitivity of this fluorescent amine to ΔpH of low extents. This is also evident from the experiments reported in Fig. 2, where it is shown that an artificially induced ΔpH of about 0.2 units promotes a 5% quenching of fluorescence in membranes containing phospholipids and proteins, corresponding to 200 μM and 400 μg, respectively.

Characterization of proton flux at the early turnovers of the hydrolase activity is crucial for understanding functional interactions between the catalytic and proton pumping sectors of the ATPase complex in energy coupling membranes. In earlier experiments, working with eosin-labeled chromatophores on F_1, we measured that the lifetime of the light-induced conformational change of the catalytic sector during activity was in the range of 100 ms [42]. Assuming this figure as a reliable time also for the enzyme turnover in the dark, it appears that ACMA is particularly suited to detect transmembrane proton flow sustained by the ATPase activity. The response time of this probe to ΔpH formation was indeed evaluated in the range of 70 ms at 27°C (as detected with a rapid mixing technique) [21]. Due to the hydrophobicity of the molecule [43], the use of Eqn. 2 to compute ΔpH from the time course of the quenching of fluorescence sets on the notion that the time of equilibrium redistribution of the probe between the water and the membrane phase is negligible, as compared to ΔpH generation.

Furthermore, the coincidence of K_m for the substrates, as well as the parallel effect detected when activators and/or inhibitors of the hydrolase were tested on both the hydrolytic and proton pumping activities, strongly support the conclusion that the fluorescent probe used in this study is competent to monitor proton flux and transmembrane ΔpH generated by the catalytic activity of the F_1 sector of the membrane-integrated ATPase complex.

In our experiments the multiple equilibria of ion–adenine nucleotide complexes are considered in order to determine the $MgATP^{2-}$ concentration. This species, which, according to Eqn. 1, is predominant at pH 8.5, when ATP and Mg^{2+} are added at equimolar concentrations, in the absence of ADP and AMP concentrations except those arising from ATP contamination, is considered the effective substrate for ATPase activity, which is optimal at this pH [12]. The use of Eqn. 1 is, however, recommended in evaluating the effective substrate concentration, since this may be up to 20% less than that of the total added concentration under the conditions previously outlined. When this is considered in kinetic analysis, it appears that the ATPase activity of dark adapted chromatophores is activated by substrate addition in parallel with the ATP-dependent proton pump, and that the ΔpH generation is modulated simultaneously with modulation of the ATP hydrolase at the catalytic site(s). This is confirmed also by the inhibitory and stimulatory effects on both activities observed in the presence of excess Mg^{2+}, with respect to substrates or sulphite, even at low concentrations. Taken together, these data indicate a close functional relationship between the catalytic site(s) on F_1 and the membrane sector (F_0) of the ATPase and that, under the experimental conditions used in this work, no functional slippage in the energy coupling process is present.

Acknowledgements

The authors are indebted to Prof. B.A. Melandri for his interest during the work and stimulating discussions. This work was supported by the Italian Centre

for Research (C.N.R.) and by the Italian Ministero della Ricerca Scientifica.

References

1 Casadio, R., Baccarini Melandri, A. and Melandri, B.A. (1974) FEBS Lett. 49, 203–207.
2 Baccarini Melandri, A., Casadio, R. and Melandri, B.A. (1981) Curr. Top. Bioenerg. 12, 197–258.
3 Mitchell, P. (1985) FEBS Lett. 82, 1–7.
4 Boyer, P.D (1989) FASEB J. 3, 2164–2178.
5 Stein, W.D. and Läuger, P. (1990) Biophys. J. 57, 255–267.
6 Fillingame, R.H. (1990) in The Bacteria: A Treatise on Structure and Functioning (Krulwich, T.A., ed.), Vol. 12, pp. 343–391, Academic Press, New York.
7 Senior, A.E. (1990) Annu. Rev. Biophys. Biophys. Chem. 19, 7–41.
8 Futai, M., Noumi, T. and Maeda, M. (1989) Annu. Rev. Biochem. 58, 111–136.
9 Gabellini, N., Gao, Z., Eckerskorn, C., Lottspeich, F. and Oesterhelt D. (1988) Biochim. Biophys. Acta 934, 227–234.
10 Glaser, E. and Norling, B. (1991) Curr. Top. Bioenerg. 16, 223–263.
11 Hoppe, J. and Sebald, W. (1984) Biochim. Biophys. Acta 768, 1–27.
12 Baccarini Melandri, A. and Melandri, B.A. (1978) in The Photosynthetic Bacteria (Clayton, R.K. and Sistrom. W.R., eds.), pp. 615–628, Plenum Press, New York.
13 Strotmann, H. and Bickel-Sandkotter, S. (1984) Annu. Rev. Plant Physiol. 35, 97–120.
14 Gräber, P. (1990) in Bioelectrochemistry III (Milazzo, G. and Balnk, M., eds.), pp. 277–309, Plenum Press, New York.
15 Casadio, R. and Melandri B.A. (1984) in H^+-ATPase: Structure, Function, Biogenesis. The F_0–F_1 Complex of Coupling Membranes (Papa, S., Altendorf, K., Ernster, L. and Packer, L., eds.), pp. 411–420, ICSU Press, Adriatica Editrice, Bari.
16 Turina, P., Rumberg, B., Melandri, B.A. and Gräber, P. (1992) J. Biol. Chem. 267, 11057–11063.
17 Webster, G.D., Edwards, P.A. and Jackson, J.B. (1977) FEBS Lett. 76, 29–35.
18 Casadio, R. (1988) in The Ion Pumps. Structure, Function and Regulation (Stein, W.D., ed.), pp. 201–206, Alan R. Liss, New York.
19 Gromet-Elhanan, Z. and Weiss, S. (1989) Biochemistry 28, 3645–3650.
20 Engelbrecht, S. and Junge, W. (1990) Biochim. Biophys. Acta 1015, 379–390.
21 Casadio, R. (1991) Eur. Biophys. J. 19, 189–201.
22 Baccarini Melandri, A. and Melandri, B.A. (1971) Methods Enzymol. 123, 556–561.
23 Clayton, R.K. (1963) Biochim. Biophys. Acta 75, 312–323.
24 Baccarini Melandri, A., Casadio R. and Melandri B.A. (1977) Eur. J. Biochem. 78, 389–402.
25 Taussky, H. and Schorr, J. (1951) J. Biol. Chem. 202, 675–680.
26 Orange, M. and Rhein, H.C. (1951) J. Biol. Chem. 18, 379–386.
27 Dito, W.R. (1976) Ann. J. Clin. Pathol. 65, 1016–1018.
28 Glaser, E., Norling, B. and Ernster, L. (1980) Eur. J. Biochem. 110, 225–235.
29 Casadio, R. and Melandri, B.A. (1985) Arch. Biochem. Biophys. 238, 219–228.
30 Press, W.H., Flannery, P.P., Teukolsky, S.A. and Vetterlin, W.T. (1986) Numerical Recipes, Cambridge University Press, London.
31 Perrin, D.D. (1965) Nature 206, 170–171.
32 Storer, A.C. and Cornish-Bowden, A. (1976) Biochem. J. 159, 1–5.
33 Pecoraro, V.L., Hermes, J.D. and Cleland, W.W. (1984) Biochemistry 23, 5262–5271.
34 Phillips, R.C., George, P. and Rutman, R.J. (1966) J. Am. Chem. Soc. 88, 2631–2640.
35 Adolfsen, R. and Moudrianakis, E.N. (1977) J. Biol. Chem. 253, 4378–4379.
36 Gajewski, E., Steckler, D.K. and Goldberg, R.N. (1986) J. Biol. Chem. 261, 12733–12737.
37 Smith, M.R. and Martell, A.E. (1975) Critical Stability Constants, Vol. 2, Plenum Publ. Co., London.
38 Bevington, P.R. (1969) Data Reduction and Error Analysis for the Physical Science, McGraw-Hill Inc., New York.
39 Kraayenhof, R. (1980) Methods Enzymol. 69, 510–520.
40 Haraux, F. and de Kouchkovsky, Y. (1980) Biochim. Biophys. Acta 592, 153–168.
41 Schuldiner, S., Rottenberg, H. and Avron, M. (1972) Eur. J. Biochem. 1972, 64–70.
42 Casadio, R. and Wagner, R. (1985) Biochim. Biophys. Acta 809, 215–227.
43 Marty, A., Bourdeaux, M., Dell'Amico, M. and Viallet, P. (1989) Eur. Biophys. J. 13, 251–257.